Stochastic Dynamic Pricing for EV Charging Stations With Renewable Integration and Energy Storage

Chao Luo, Yih-Fang Huang, *Fellow, IEEE*, and Vijay Gupta, *Member, IEEE*

***Abstract*—This paper studies the problem of stochastic dynamic pricing and energy management policy for electric vehicle (EV) charging service providers. In the presence of renewable energy integration and energy storage system, EV charging service providers must deal with multiple uncertainties—charging demand volatility, inherent intermittency of renewable energy generation, and wholesale electricity price fluctuation. The motivation behind our work is to offer guidelines for charging service providers to determine proper charging prices and manage electricity to balance the competing objectives of improving profitability, enhancing customer satisfaction, and reducing impact on power grid in spite of these uncertainties. We propose a new metric to assess the impact on power grid without solving complete power flow equations. To protect service providers from severe financial losses, a safeguard of profit is incorporated in the model. Two algorithms—stochastic dynamic programming (SDP) algorithm and greedy algorithm (benchmark algorithm)—are applied to derive the pricing and electricity procurement policy. A Pareto front of the multi-objective optimization is derived. Simulation results show that using SDP algorithm can achieve up to 7% profit gain over using greedy algorithm. Additionally, we observe that the charging service provider is able to reshape spatial-temporal charging demands to reduce the impact on power grid via pricing signals.**

***Index Terms*—Electric vehicle, charging station, dynamic pricing, energy management, renewable energy, energy storage, multi-objective optimization, stochastic dynamic programming.**

Nomenclature

K	Total number of planning horizons.
N	Number of buses in a power network.
M	Number of PQ buses in a power network.
s_j	The j-th charging station.
p_{kj}	Charging price of the j-th charging station at the k-th horizon.
d_{kj}	Charging demand of the j-th charging station at the k-th horizon.
c_k	Real time wholesale electricity price at the k-th horizon.
E	Electricity storage capacity.
I_k	Remaining electricity in storage at the beginning of the k-th horizon.
W_k	Profit at the k-th horizon.
$W_{\min}$	Threshold for profit safeguard.
G_k	Customer satisfaction at the k-th horizon.
F_k	Impact on power grid at the k-th horizon.
o_k	Electricity purchase at the k-th horizon.
u_k	Renewable energy at the k-th horizon.
η_s	Unit storage cost (measured in \$/MWh).
η_c	Charging efficiency.
η_d	Discharging efficiency.
α	Shape parameter in customer satisfaction formula.
ω	Shape parameter in customer satisfaction formula.
ϕ_k	Total charging demand at the k-th horizon.
Π_k	Total utility at the k-th horizon.
λ_1	Profit weight coefficient.
λ_2	Customer satisfaction weight coefficient.
λ_3	Impact weight coefficient.
$\gamma_{i,j}$	Price elasticity coefficient.
P_i	Active power of the i-th bus.
Q_i	Reactive power of the i-th bus.
v_i	Voltage magnitude of the i-th bus.
δ_i	Voltage phase of the i-th bus.
G_{ik}	Conductance of the ik-th element of the bus admittance matrix.
B_{ik}	Susceptance of the ik-th element of the bus admittance matrix.
S_i^{Ac}	Active power sensitivity of the i-th bus.
S_i^{Re}	Reactive power sensitivity of the i-th bus.
$J(I_k, u_k)$	Maximum expected aggregated utility from the k-th horizon to the k-th horizon.

Manuscript received June 22, 2016; revised November 12, 2016 and February 16, 2017; accepted March 29, 2017. Date of publication April 24, 2017; date of current version February 16, 2018. This work was supported by the National Science Foundation under Grant CNS-1239224, Grant ECCS-1550016, and Grant CPS-1544724. This paper was presented, in part, at the 2nd International Conference on Vehicle Technology and Intelligent Transport Systems. Paper no. TSG-00838-2016. *(Corresponding author: Chao Luo.)*

C. Luo, Y.-F. Huang, and V. Gupta are with the Department of Electrical Engineering, University of Notre Dame, Notre Dame, IN 46556 USA (e-mail: cluo1@nd.edu; huang@nd.edu; vgupta2@nd.edu).

Color versions of one or more of the figures in this paper are available online at http://ieeexplore.ieee.org.

Digital Object Identifier 10.1109/TSG.2017.2696493

I. Introduction

ELECTRIC vehicles (EVs) exhibit many advantages over fossil fuel driven vehicles in terms of operation and maintenance cost, energy efficiency, and gas emission [1]–[3]. However, the fear of limited driving distance (range anxiety) is hanging over EV drivers' heads like the Sword of Damocles. To alleviate this range anxiety, the capacity of on-board battery should be increased and more EV charging stations should be deployed. Intensive research work has been carried out to study how to strategically deploy charging stations [4]–[8]. Currently, EV charging service is primarily provided for free as one of the employee benefits in some organizations or as a perk to those owners of some specific EV models (e.g., Tesla). There is a lack of viable and profitable pricing and energy management model for public charging stations. Our goal is to offer guidelines for charging service providers to make informed and insightful decisions on pricing and electricity procurement by jointly optimizing multiple objectives under uncertainties.

There is a growing literature aimed at providing guidelines for economic operation of EV charging stations. Guo *et al.* [9], [10] studied a dynamic pricing scheme to improve the revenue of an EV parking deck. However, their model did not take into account customer satisfaction and the impact on power grid due to EV charging. In [11]–[14], several algorithms have been proposed for a power aggregator to manage EV charging loads and submit bids to electricity market to provide regulation service (RS). Game theory based approaches have been used to model the interplay among multiple EVs or between EVs and power grid in [15]–[18]. Yan *et al.* [19] presented a multi-tier real time pricing algorithm for EV charging stations to encourage customers to shift their charging schedule from peak period to off-peak period. Nevertheless, they did not consider that some customers may strategically change their charging schedule in response to pricing signals. Ban *et al.* [20] employed multi queues to model the arrivals and departures of EVs among multiple charging stations. Pricing signals were used to guide EVs to different charging stations to satisfy the predefined quality of service (QoS); but the interactions between EV charging and power grid was not analysed in their model. A distributed network cooperative method was proposed to minimize the charging cost of EVs while guaranteeing that the aggregated load satisfies safety limits [21]. Their model, however, did not incorporate renewable energy generation and consider charging demand volatility.

In our model, we take a comprehensive view of these interweaving issues pertaining to EV charging pricing and energy management. Specifically, we formulate our problem to simultaneously optimize multiple objectives — improving the profit, enhancing the customer satisfaction, and reducing the impact on power grid in the light of renewable energy generation and energy storage. Our model takes into account multiple uncertainties including charging demand volatility, inherent intermittency of renewable energy generation, and real time wholesale electricity price fluctuation. For each type of uncertainty, an appropriate model is proposed and incorporated in the overall optimization framework. Finally, a stochastic dynamic programming (SDP) algorithm is employed to derive the charging prices and the electricity procurement from the power grid for each planning horizon. Besides, SDP algorithm has been used for water reservoir operation in [22] and [23]. In terms of the electricity retail market, a game theory based dynamic pricing scheme is studied in [24] which also takes into account renewable integration and local storage.

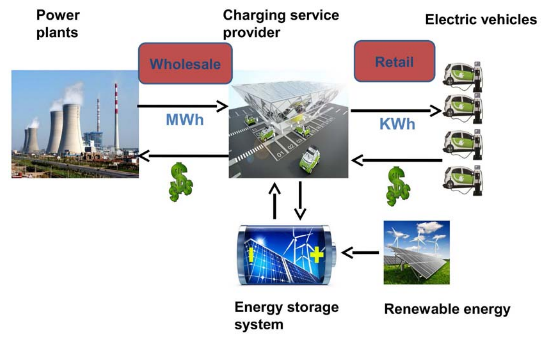

Fig. 1. Business Model of EV Charging Service Provider.

The main contributions of our work are as follows:

- We proposed a multi-objective optimization framework to solve the problem, and the solutions provide us insights into how to make a tradeoff among multiple objectives of the profitability, the customer satisfaction, and impact on power grid, and offer guidance to set charging prices to balance the charging demand across the power system.
- We used Newton's method to derive a fast-computing metric to assess the impact of EV charging on power grid, which frees us from solving the complete nonlinear power flow equations. This metric also can be used to analyze other electric load's impact on power grid.
- We derived the active power and reactive power sensitivities for the load buses in a power system which can serve as a guideline for EV charging station placement to alleviate the charging stress on the power grid.
- In terms of market risk, we introduced a safeguard of profit for EV charging service providers, which raises a warning when the profit is likely to reach a dangerous threshold. This mechanism is beneficial for the charging service provider to safely manage its capital and avoid severe financial losses.

The remainder of the paper is organized as follows: Section II presents the general problem formulation. Section III introduces charging demand estimation and Section IV discusses how to assess the impact on power grid from EV charging. Renewable energy and real time wholesale electricity price forecast, the safeguard of profit, and SDP algorithm are introduced in Section V. Section VI presents simulation results and discussions. Conclusions are provided in Section VII. A nomenclature table is also provided as a reference.

II. Problem Formulation

In this study, we assume that an EV charging service provider operates a set of charging stations within a large region. As a mediator between the wholesale market and end customers (EVs), the charging service provider procures electricity from the wholesale market and resells it to EVs. We also assume that the service provider is able to harvest renewable energy (i.e., solar or wind power) and save it in an energy storage system. An overview of the EV charging service provider's model is illustrated in Fig. 1.

A. Profit of Charging Service Provider

In the United States, the Independent System Operator (ISO) or the Regional Transmission Organization (RTO) collects supply offers from power plants and demand bids from load serving entities (LSEs) or market participants, calculates the day-ahead wholesale prices and real time spot prices, coordinates and monitors the economic dispatch of electricity across a vast region [25]–[27]. We assume that the charging service provider is an LSE, who purchases electricity from the wholesale real time market and resells it to EVs. Let $\mathcal{S} = \{s_1, s_2, \ldots, s_L\}$ denote the charging stations operated by the service provider. A day is divided into K planning horizons. At the start of each horizon, the service provider will publish new charging prices during this horizon. Price differentiation is allowed across charging stations. Let $\mathcal{P} = \{p_{k1}, p_{k2}, \ldots, p_{kL}\}, k = 1, 2, \ldots, K$ denote the charging prices in the k-th horizon, and o_k denote electricity procurement from the wholesale real time market. We use wholesale real time electricity market prices in our theoretical analysis. Let $\mathcal{C} = \{c_1, c_2, \ldots, c_K\}$ represent wholesale real time electricity prices. In addition, we assume that the service provider has an energy storage system with capacity E MWh. Let I_k denote the electricity in the storage at the beginning of the k-th horizon, and u_k be the renewable energy generation during the k-th horizon. The profit made in the k-th horizon is given by

$$W_k = \sum_{j=1}^{L} p_{kj} d_{kj} - c_k o_k - \eta_s \left(I_k + \eta_c u_k + \eta_c o_k - \frac{1}{\eta_d} \sum_{j=1}^{L} d_{kj} + w_k \right), \tag{1}$$

where d_{kj} corresponds to the charging demand (electricity consumption) at the j-th station in the k-th horizon, $\sum_{j=1}^{L} p_{kj} d_{kj}$ is the total revenue, $c_k o_k$ is the cost of electricity procurement, and η_s(\$/MWh) is the unit storage cost, which includes capital cost and maintenance cost. Besides, η_c $(0 < \eta_c < 1)$ and η_d $(0 < \eta_d < 1)$ are charging efficiency and discharging efficiency, respectively. And w_k is the process noise of the energy storage system, which has a Gaussian distribution with zero mean and variance σ_w^2.

B. Customer Satisfaction

Customer satisfaction helps to build up customer loyalty, which can reduce the efforts to allocate market budgets to acquire new customers. Poor customer satisfaction will discourage people to purchase EVs, affecting the development of entire EV industry. Customer satisfaction is one of the objectives in our multi-objective optimization framework. Several customer satisfaction evaluation methods have been investigated in [28]–[30]. In this paper, we consider the market-level customer satisfaction instead of the individual-level satisfaction. We use a quadratic function to formulate the overall customer satisfaction of all EVs in a horizon, namely,

$$G_k = -\frac{\alpha}{2} \phi_k^2 + \omega \phi_k, \; 0 \leq \phi_k \leq E \tag{2}$$

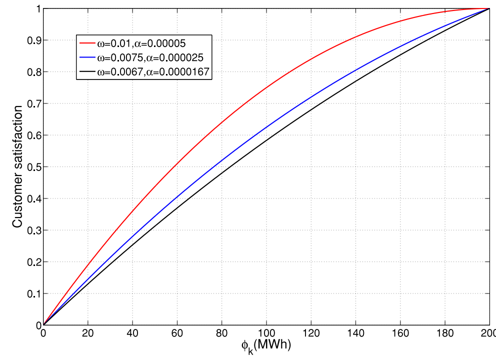

Fig. 2. Sample Customer Satisfaction Functions ($E = 200$).

where E is the electricity storage capacity, ω and α are shape parameters, ϕ_k is the aggregated charging demand (electricity consumption) of all EVs in the k-th horizon which is defined as,

$$\phi_k = \sum_{j=1}^{L} d_{kj}. \tag{3}$$

Eq. (2) with different shape parameters is plotted in Fig. 2. In plotting Fig. 2, we choose the shape parameters α and ω such that the concave function G_k has a minimum of 0, which indicates that EV drivers have the least satisfaction, and a maximum of 1, which indicates that they have the most satisfaction. Note that Eq. (2) is a non-decreasing function with a non-increasing first order derivative. This implies that customer satisfaction will always grow as the total charging demand ϕ_k increases, but the growth rate will decrease and customer satisfaction tends to get saturated as the total charging demand approaches the storage capacity E. This is a standard assumption following the law of diminishing marginal utility (Gossen's First Law) in economics [31].

C. Impact on Power Grid

Large-scale EV charging presents a substantial load to power networks [32], [33]. Many studies have shown that uncoordinated EV charging can affect the normal operation of power grid in terms of severe power loss, voltage variation, frequency deviation, and harmonics problems [34]–[38]. Usually, grid frequency can be well maintained either by the power generator side using automatic gain control (AGC) [37] or by the load side using certain demand response techniques [39], [40]. In our study here, we only consider the impact of voltage variation (magnitude and phase). In addition, we assume that a higher-level entity like an aggregator or ISO/RTO can take care of network transmission constraint issues within the power system under its supervision, so the EV charging service provider does not need to worry about transmission constraint problem. Let F_k denote the impact of EV charging on power grid at the k-th horizon.

$$F_k = f(d_{k1}, d_{k2}, \ldots, d_{kL}), \tag{4}$$

where d_{kj} is the charging demand at the j-th charging station in the k-th horizon, and $f(.)$ is a function to be discussed in Section IV. Function $f(.)$ should reflect the basic assumption that the impact on power grid increases when the charging demands increase.

D. Multi-Objective Optimization Framework

A multi-objective optimization problem arises naturally from the fact that the charging service provider needs to balance multiple competing objectives — maximizing profit, maximizing customer satisfaction, and minimizing the impact on power grid. For the k-th horizon, we formulate the multi-objective optimization as follows,

$$\begin{aligned} &\max_{\mathbf{X}_k} \quad \{\mathbb{E}(W_k), \mathbb{E}(G_k), \mathbb{E}(-F_k)\} \\ &\text{s.t.} \quad \mathbf{X}_k \in U(\mathbf{X}_k), \end{aligned} \tag{5}$$

where $\mathbf{X}_k = [p_{k1}, p_{k2}, \ldots, p_{kL}, o_k]^{\mathrm{T}}$ is the vector of decision variables, and $\mathbb{E}(.)$ represents the expectation operation.

Clearly, there are several approaches to solve multi-objective optimization problems: weighted sum approach, adaptive weighted sum approach, ϵ-constraint approach, a priori approach and a posteriori approach [41]–[43], among others. The weighted sum approach is not suitable for obtaining the whole Pareto front if the main objective function is not convex. In this paper, we use an adaptive weighted sum approach discussed in [43] to derive the Pareto front of Eq. (5). The main idea of the adaptive weighted sum approach is that firstly we use the ordinary weighted sum to obtain the basic shape of Pareto front, and then refine it by recursively reducing mesh size within the Pareto front. First, we rewrite the problem as follows,

$$\begin{aligned} &\max_{\mathbf{X}_k} \ \mathbb{E}(\Pi_k) = \mathbb{E}\left\{\lambda_1 \frac{W_k}{W_k^{\max}} + \lambda_2 \frac{G_k}{G_k^{\max}} - \lambda_3 \frac{F_k}{F_k^{\max}}\right\} \\ &\text{s.t.} \ \mathbf{X}_k \in U(\mathbf{X}_k), \end{aligned} \tag{6}$$

where λ_1, λ_2, and λ_3 are nonnegative coefficients, satisfying the constraint of $\lambda_1 + \lambda_2 + \lambda_3 = 1$. Different weight vectors $(\lambda_1, \lambda_2, \lambda_3)$ generates different convex Pareto optima. The non-convex part of this Pareto front can be found in the refinement phase. Additionally, $W_k^{\max}$, $G_k^{\max}$, and $F_k^{\max}$ are the maximum values of each objective function in the k-th horizon.

Our ultimate goal is to maximize the aggregated utility across multiple horizons.

$$\begin{aligned} &\left(\mathbf{X}_1^*, \ldots, \mathbf{X}_K^*\right) = \underset{\mathbf{X}_1,\ldots,\mathbf{X}_K}{\operatorname{argmax}} \left\{\sum_{k=1}^{K} \mathbb{E}(\Pi_k)\right\}, \\ &\text{s.t.} \ \mathbf{X}_k \in U(\mathbf{X}_k), k = 1, 2, \ldots, K. \end{aligned} \tag{7}$$

To solve this multi-horizon and multi-objective optimization problem, we face several challenges: (1) How do we accurately estimate the charging demand d_{kj} at each charging station? (2) How do we develop an appropriate metric to assess the impact on power grid defined in Eq. (4)? (3) How should we incorporate a safeguard of profit to prevent severe financial losses? (4) How can we solve this complex optimization problem in an efficient manner? In the following sections, we will address these challenges in details.

III. Charging Demand Estimation

In practice, EV drivers will adjust their charging demands and charging schedules in response to charging prices. The charging demand function d_{kj} thus should characterize customers' response to price fluctuations. In our work, an online linear regression model [44], [45] is employed to predict the charging demand d_{kj}. For each charging station, the predicted charging demand is defined as

$$\begin{cases} d_{k1} = \gamma_{0,1} - \gamma_{1,1}p_{k1} + \gamma_{2,1}p_{k2} + \ldots + \gamma_{L,1}p_{kL} + \epsilon_{k1}, \\ d_{k2} = \gamma_{0,2} + \gamma_{1,2}p_{k1} - \gamma_{2,2}p_{k2} + \ldots + \gamma_{L,2}p_{kL} + \epsilon_{k2}, \\ \vdots \\ d_{kL} = \gamma_{0,L} + \gamma_{1,L}p_{k1} + \gamma_{2,2}p_{k2} + \ldots - \gamma_{L,L}p_{kL} + \epsilon_{kL}, \end{cases} \tag{8}$$

where $\gamma_{0,j} (j = 1, 2, \ldots, L)$ is the intercept of the j-th linear regression equation, $\gamma_{i,j} = \gamma_{j,i} (i \neq j)$ are the cross-price elasticity coefficients, reflecting how the change of the charging price at station j can influence the charging demand at station i, and $\gamma_{i,i}$ is the self-price elasticity coefficient, reflecting how the change of the charging price of station i can influence its own charging demand. Finally $\epsilon_{kj} (j = 1, 2, \ldots, L)$ is assumed to be an independent Gaussian random variable with mean 0 and variance σ_{kj}^2. The variable ϵ_{kj} captures the unknown random charging demand which cannot be characterized by the linear terms.

Recursive least square (RLS) algorithm is a common method applied to estimate the coefficients in Eq. (8) using historical data [46], [47]. Let $\mathbf{Y}_j = [\gamma_{0,j}, \gamma_{1,j}, \ldots, \gamma_{L,j}]^{\mathrm{T}}$ denote the vector of price elasticity coefficients related to the j-th charging station. Applying RLS, we have the following update equations,

$$\begin{cases} e_{kj} = d_{kj} - \mathbf{P}_k^{\mathrm{T}}\mathbf{Y}_j, \\ g_{kj} = \frac{\mathbf{H}_{(k-1)j}\mathbf{P}_k}{\nu + \mathbf{P}_k^{\mathrm{T}}\mathbf{H}_{(k-1)j}\mathbf{P}_k}, \\ \mathbf{H}_{kj} = \nu^{-1}\mathbf{H}_{(k-1)j} - g_{kj}\mathbf{P}_k^{\mathrm{T}}\nu^{-1}\mathbf{P}_k, \\ \mathbf{Y}_j \leftarrow \mathbf{Y}_j + e_{kj}g_{kj}, \end{cases} \tag{9}$$

where ν is the forgetting factor. Besides, H_{0j} is initialized to be an identity matrix and P_0 is initialized to be an all-zero vector. In addition, the estimate for variance σ_{kj}^2 is given by

$$\begin{cases} m_{kj} = \nu m_{(k-1)j} + \epsilon_{kj}, \\ n_{kj} = \nu n_{(k-1)j} + 1, \\ \bar{\epsilon}_{kj} = m_{kj}/n_{kj}, \\ u_{kj} = \left(\frac{m_{kj}-1}{m_{kj}}\right)^2 + \left(\frac{1}{m_{kj}}\right)^2, \\ v_{kj} = m_{kj}(1 - u_{kj}), \\ \sigma_j^2 \leftarrow \frac{1}{v_{kj}}\left[\left(\nu v_{kj}\right)\sigma_j^2 + \frac{m_{kj}-1}{m_{kj}}\left(\bar{\epsilon}_{kj} - \epsilon_{kj}\right)^2\right], \end{cases} \tag{10}$$

where m_{kj} and n_{kj} are initialized to be 0.

Eq. (8) can characterize the spatial-temporal variation of charging demand. Different locations may have different charging demands. Thus, we use different linear regression equations to model these geographically separated charging stations. Furthermore, the price elasticity coefficients are updated continually using RLS algorithm defined in Eq. (9) and Eq. (10). The forgetting factor ν enables us to capture the most recent trend in charging demand and forget the outdated information. Thus, the RLS updating mechanism is able to track charging demand fluctuation over time.

IV. Impact on Power Grid From EV Charging

For power flow analysis, we assume that an N-bus power network has 1 slack bus, M load buses (PQ buses), and $N-M-1$ voltage-controlled buses (PV buses) [48]. Three phase balance operation and per-unit (p.u.) system are basic assumptions here. Charging stations are deployed across different PQ buses. Solving the power flow requires determining $N-1$ voltage phases (corresponding to PQ buses and PV buses) and M voltage magnitude (corresponding to PQ buses). This is done by solving $N+M-1$ nonlinear power flow equations ($N-1$ active power equations and M reactive power equations). The active and reactive power flow equations for each bus are given as follows,

$$P_i = v_i \sum_{k=1}^{N} v_k (G_{ik} \cos(\delta_i - \delta_k) + B_{ik} \sin(\delta_i - \delta_k)), \quad (11)$$

$$Q_i = v_i \sum_{k=1}^{N} v_k (G_{ik} \sin(\delta_i - \delta_k) - B_{ik} \cos(\delta_i - \delta_k)), \quad (12)$$

where v_i and δ_i are, respectively, voltage magnitude and phase at the i-th bus; P_i and Q_i are real power and reactive power injections at the i-th bus; G_{ik} and B_{ik} are, respectively, conductance and susceptance of the ik-th element of the bus admittance matrix.

An increasing EV charging demand at PQ buses will lead to network-wide voltage variation (magnitude and phase) if the network does not provide sufficient active power and reactive power. We will use voltage variation as a metric to assess the impact of EV charging on power grid. Applying Newton's method, we can calculate the linear approximation of voltage variation in the following way

$$\begin{bmatrix} \mathbf{\Delta V} \\ \mathbf{\Delta \Phi} \end{bmatrix} = \begin{bmatrix} \frac{\partial \mathbf{P}}{\partial \mathbf{V}} & \frac{\partial \mathbf{P}}{\partial \mathbf{\Phi}} \\ \frac{\partial \mathbf{Q}}{\partial \mathbf{V}} & \frac{\partial \mathbf{Q}}{\partial \mathbf{\Phi}} \end{bmatrix}^{-1} \begin{bmatrix} \mathbf{\Delta P} \\ \mathbf{\Delta Q} \end{bmatrix} = \mathbf{J}^{-1} \begin{bmatrix} \mathbf{\Delta P} \\ \mathbf{\Delta Q} \end{bmatrix}, \quad (13)$$

where $\mathbf{\Delta V}$ and $\mathbf{\Delta \Phi}$ are, respectively, vectors of magnitude variation and phase variation; $\mathbf{\Delta P}$ and $\mathbf{\Delta Q}$ are, respectively, vectors of increased active power and reactive power due to EV charging. In addition, $\frac{\partial \mathbf{P}}{\partial \mathbf{V}}$ and $\frac{\partial \mathbf{P}}{\partial \mathbf{\Phi}}$ are partial derivatives of active power with respect to voltage magnitudes and phases, and $\frac{\partial \mathbf{Q}}{\partial \mathbf{V}}$, $\frac{\partial \mathbf{Q}}{\partial \mathbf{\Phi}}$ are partial derivatives of reactive power with respect to voltage magnitudes and phases. In addition, $\mathbf{J}^{-1}$ is the inverse of Jacobian matrix from power flow equations, which is given by

$$\mathbf{J}^{-1} = \begin{bmatrix} b_{1,1} & b_{1,2} & \dots & b_{1,N+M-1} \\ b_{2,1} & b_{2,2} & \dots & b_{2,N+M-1} \\ \vdots & & & \vdots \\ b_{N+M-1,1} & b_{N+M-1,2} & \dots & b_{N+M-1,N+M-1} \end{bmatrix}, \quad (14)$$

Let the sequence $[a_1, a_2, \dots, a_L]$ denote the bus indexes of all charging stations in the power network. For instance, $a_i (i = 1, 2 \dots, L)$ means that the i-th charging station is fed by the a_i-th bus in the power network.

Finally, we use the 2-norm voltage variation (magnitude and phase) to assess the impact of EV charging on power grid,

$$F_k = \left\| \mathbf{J}^{-1} \begin{bmatrix} \mathbf{\Delta P} \\ \mathbf{\Delta Q} \end{bmatrix} \right\|^2. \quad (15)$$

Moreover, we denote S_i^{Ac} and S_i^{Re} as the active power sensitivity and reactive power sensitivity of the i-th PQ bus. And S_i^{Ac} is defined as follows,

$$S_i^{\mathrm{Ac}} = \left\| \mathbf{J}^{-1} \begin{bmatrix} 0 \\ \vdots \\ 0 \\ 1 \\ 0 \\ \vdots \\ 0 \end{bmatrix} \right\|^2, \quad (16)$$

where S_i^{Ac} is the 2-norm voltage variation when the active power injection of the i-th PQ bus is increased by 1 W. Thus, 1 W is the i-th entry in the column vector in Eq. (16). Similarly, S_i^{Re} is defined as the 2-norm voltage variation when the reactive power injection of the i-th PQ bus is increased by 1 var. A larger value of S_i^{Ac} or S_i^{Re} indicates that the PQ bus has a lower tolerance to load variation and more likely to disturb the whole network.

V. Stochastic Dynamic Programming (SDP) for Pricing and Electricity Procurement

At first, this section introduces a safeguard of profit — a minimum profit warning mechanism. In addition, major modules in SDP like renewable energy, real time wholesale electricity price, and system dynamics are discussed. Finally, we introduce the procedure to use SDP to derive pricing and electricity procurement policy.

A. A Safeguard of Profit

In practice, service providers make decisions on pricing and electricity procurement based on the estimated charging demands. Although Eq. (8) provides a viable way to estimate the charging demand, uncertainties still exist in actual charging demands. This subsection aims to develop a safeguard of profit to remind that the charging service provider should make a certain amount of profit under severe circumstance of uncertainties. We incorporate the safeguard as a constraint in the optimization framework. Wherever the optimal solution touches this constraint (i.e., this constraint becomes active), a warning will be raised for the service provider. The constraint is given as follows,

$$\mathrm{Prob}(W_k < W_{\min}) < \zeta, \quad (17)$$

where W_k is the profit made in the k-th horizon, $W_{\min}$ is a profit threshold, and ζ is a small positive number in the range of (0, 1). Eq. (17) specifies that the probability that the actual profit is less than the profit threshold should be less than ζ.

Expanding W_k and rearranging terms in Eq. (17) yields the following

$$\mathrm{Prob}\big(\mathbf{X}_k^{\mathrm{T}} \mathbf{A} \mathbf{X}_k + \mathbf{B}^{\mathrm{T}} \mathbf{X}_k + \mathbf{E}_k^{\mathrm{T}} \mathbf{Z}_k + t_k < W_{\min}\big) < \zeta, \quad (18)$$

where $\mathbf{X}_k = [p_{k1}, p_{k1}, \ldots, p_{kL}, o_k]^{\mathrm{T}}$. Matrix A is given by

$$\mathbf{A} = \begin{bmatrix} -\gamma_{1,1} & \gamma_{1,2} & \ldots & \gamma_{1,L} & 0 \\ \gamma_{2,1} & -\gamma_{2,2} & \ldots & \gamma_{2,L} & 0 \\ \vdots & \vdots & & \vdots & \vdots \\ \gamma_{L,1} & \gamma_{L,2} & \ldots & -\gamma_{L,L} & 0 \\ 0 & 0 & \ldots & 0 & 0 \end{bmatrix}, \tag{19}$$

and vector $\mathbf{B}$ is

$$\mathbf{B} = \left[\gamma_{0,1} + \frac{\eta_s}{\eta_d}\Gamma_1, \ldots, \gamma_{0,L} + \frac{\eta_s}{\eta_d}\Gamma_L, -c_k - \eta_s\eta_c\right]^{\mathrm{T}}, \tag{20}$$

where Γ_j is

$$\Gamma_j = -\gamma_{j,j} + \sum_{i=1, i\neq j}^{L} \gamma_{j,i}, \tag{21}$$

and vector E is

$$\mathbf{E}_k = \left[p_{k1} + \frac{\eta_s}{\eta_d}, \ldots, p_{kL} + \frac{\eta_s}{\eta_d}, -\eta_s\right]^{\mathrm{T}}, \tag{22}$$

and $\mathbf{Z}_k = [\epsilon_{k1}, \epsilon_{k2}, \ldots, \epsilon_{kL}, w_k]^{\mathrm{T}}$, and $t_k = \eta_s(\Gamma_0/\eta_d - I_k - \eta_c u_k)$, where Γ_0 is

$$\Gamma_0 = \sum_{i=1}^{L} \gamma_{0,i}. \tag{23}$$

Besides, we assume that $[\epsilon_{k1}, \epsilon_{k2}, \ldots, \epsilon_{kL}, w_k]^{\mathrm{T}}$ are independent Gaussian random variables. Thus, $\mathbf{E}_k^{\mathrm{T}}\mathbf{Z}_k$ is also a Gaussian random variable with mean 0 and variance $\sum_{j=1}^{L}(p_{kj} + \eta_s/\eta_d)^2\sigma_{kj}^2 + \eta_s^2\sigma_w^2$.

Finally, Eq. (17) can be rewritten as follows,

$$\begin{aligned} &\mathrm{Prob}\big(\mathbf{E}_k^{\mathrm{T}}\mathbf{Z}_k < W_{\min} - \mathbf{X}_k^{\mathrm{T}}\mathbf{A}\mathbf{X}_k - \mathbf{B}^{\mathrm{T}}\mathbf{X}_k - t_k\big) \\ &\quad = \mathbf{\Phi}\left(\frac{W_{\min} - \mathbf{X}_k^{\mathrm{T}}\mathbf{A}\mathbf{X}_k - \mathbf{B}^{\mathrm{T}}\mathbf{X}_k - t_k}{\sqrt{\sum_{j=1}^{L}\big(p_{kj} + \eta_s/\eta_d\big)^2\sigma_{kj}^2 + \eta_s^2\sigma_w^2}}\right) < \zeta, \end{aligned} \tag{24}$$

where $\mathbf{\Phi}(.)$ is the cumulative distribution function (CDF) of a standard Gaussian random variable.

B. Renewable Energy and Real Time Wholesale Price

Literature abounds on various approaches to forecasting renewable energy, e.g., physical approach [49], [50], statistical approach [51], [52], and hybrid approach [53]. In this paper, we use a Markov chain model [54], [55] which is a statistical approach, to demonstrate how renewable energy prediction is incorporated into our optimization model. In fact, other forecasting approaches can also be used in our model.

Markov chain characterizes the transition from the current renewable energy u_k to the next u_{k+1}. We discretize renewable energy into D levels, and the transition matrix at the k-th horizon is given by

$$\mathbf{T}_k = \begin{bmatrix} t_{k,1,1} & t_{k,1,2} & \ldots & t_{k,1,D} \\ t_{k,2,1} & t_{k,2,2} & \ldots & t_{k,2,D} \\ \vdots & & & \vdots \\ t_{k,D,1} & t_{k,D,2} & \ldots & t_{k,D,D} \end{bmatrix}, \tag{25}$$

where $t_{k,i,j}$ is the transition probability of renewable energy from level i to level j in the k-th horizon, and $\sum_{j=1}^{D} t_{k,i,j} = 1$. All transition probabilities can be estimated from historical data.

Similar to renewable energy, real time wholesale price forecasting has also been extensively studied through time series analysis, machine learning, big data, or hybrid approach in [56] and [57]. Real time price forecasting is a topic beyond the technical scope of our paper. Thus, we do not study specific real time price forecasting approaches in this paper.

C. Stochastic Dynamic Programming

Eq. (7) is a complex multi-variable optimization problem involving $K(L+1)$ variables. It may be mathematically cumbersome and difficult to solve in a brute-force manner. We observe that the original problem exhibits the properties of overlapping subproblems and optimal substructure, which can be solved efficiently using SDP. SDP solves a large-scale complex problem by partitioning it into a set of smaller and simpler subproblems [58], [59]. The solution to the original problem is constructed by solving and combining the solutions of subproblems in a forward or backward manner. In contrast to a brute-force algorithm, SDP can greatly reduce computation and save storage.

In a wholesale real time electricity market, electricity is sold on an hourly basis. So our problem should have a finite number of planning horizons with $K = 24$. System dynamics are governed by the evolution of system states, under the influence of decision variables and random variables. In our case, system dynamics are expressed by the following equations

$$I_{k+1} = I_k + \eta_c u_k + \eta_c o_k - \frac{1}{\eta_d}\phi_k + w_k, \; u_{k+1} = h(u_k, \upsilon_k), \tag{26}$$

where I_k represents electricity storage at the beginning of the k-th horizon, u_k is renewable energy, o_k is the electricity procurement, η_c is the charging efficiency, η_d is the discharging efficiency, and ϕ_k is the total charging demand. Besides, w_k and υ_k are independent process noises for the energy storage system and the renewable energy generation.

The aggregated expected utility from the first horizon to the K-th horizon is given by

$$\mathbb{E}\left\{\Pi_{K+1}(I_{K+1}, u_{K+1}) + \sum_{k=1}^{K}\Pi_k(I_k, u_k)\right\}, \tag{27}$$

where $\Pi_{K+1}(I_{K+1}, u_{K+1})$ is a terminal utility occurred at the end of this process, and the expectation is taken over $\epsilon_{kj} (j = 1, \ldots, L)$ defined in Eq. (8), w_k, and υ_k. Therefore, the maximum aggregated expected utility $J(I_1, u_1)$ is given by

$$J_1(I_1, u_1) = \max_{\mathbf{X}_1, \ldots, \mathbf{X}_K} \mathbb{E}\left\{\Pi_{K+1} + \sum_{k=1}^{K}\Pi_k\right\},$$

$$s.t. \begin{cases} \text{Prob}(W_k < W_{\min}) < \zeta \\ 0 \le o_k \le o_{\max};\ k = 1, 2, \ldots, N \\ p_{kj} \ge 0;\ j = 1, 2, \ldots, L \\ I_k + u_k + o_k - \sum_{j=1}^{L} d_{kj} \ge 0 \\ I_k + u_k + o_k - \sum_{j=1}^{L} d_{kj} \le E \\ d_{kj} \ge 0;\ j = 1, 2, \ldots, L. \end{cases} \tag{28}$$

Applying SDP we can partition the problem into multiple small subproblems, which can be calculated recursively as follows,

$$\begin{aligned} J_k(I_k, u_k) &= \max_{\mathbf{X}_k \in U_k(\mathbf{X}_k)} \mathbb{E}\{\Pi_k + J_{k+1}(I_{k+1}, u_{k+1})\} \\ &= \max_{\mathbf{X}_k \in U_k(\mathbf{X}_k)} \{\mathbb{E}\{\Pi_k(I_k, u_k)\} + \mathbb{E}\{J_{k+1}(I_{k+1}, u_{k+1})\}\}. \end{aligned} \tag{29}$$

Furthermore, we can rewrite each subproblem into a nice quadratic form by combining like terms as follows,

$$J_k(I_k, u_k) = \max_{\mathbf{X}_k \in U_k(\mathbf{X}_k)} \left\{\mathbb{E}\left\{\frac{1}{2}\mathbf{X}_k^{\mathrm{T}}\mathbf{Q}\mathbf{X}_k + \mathbf{B}_k^{\mathrm{T}}\mathbf{X}_k\right\} + \mathbb{E}\{r_k\}\right\}, \tag{30}$$

where $\mathbf{Q}$, $\mathbf{B}_k$, and r_k are given by (31), (32), and (33) are shown in bottom of this page.

where $\Theta_{n,j}$ is

$$\Theta_{n,j} = -b_{j,a_n}\gamma_{n,n} + \sum_{i=1, i\neq n}^{L} b_{j,a_i}\gamma_{i,n}, \tag{34}$$

and a_n is the bus index of the power network for the n-th charging station, and

$$\Theta_{0,j} = \sum_{i=1}^{L} b_{j,a_i}\gamma_{0,i}. \tag{35}$$

Finally, $J_{k+1}(I_{k+1}, u_{k+1})$ is the total aggregated utility starting from the $(k+1)$-th horizon to the K-th horizon. Fig. 3 illustrates the schematic of the entire optimization framework.

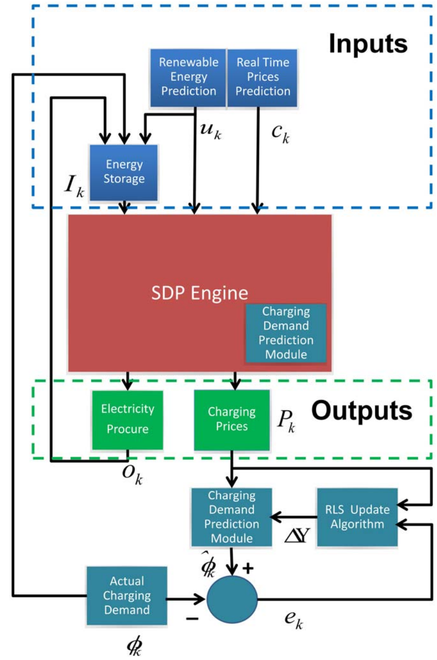

Fig. 3. Dynamic Pricing and Energy Management Algorithm.

The charging service provider should run the SDP engine at the beginning of every planning horizon.

VI. Simulations and Discussion

The simulation coefficients are given in Table I. Tesla's home rechargeable Lithium-ion battery system — Powerwall has a 92.5% round-trip DC efficiency with 100% depth of discharge [60]. Eos Energy Storage has a battery-based energy storage with a round-trip efficiency of 75% and a 100% depth of discharge [61]. In our simulation, we assume the charging efficiency η_c and discharging efficiency η_d are both 0.9. For simplicity, we use the day-ahead wholesale electricity price

$$\mathbf{Q} = \begin{bmatrix} -2\gamma_{1,1}\lambda_1 - \alpha\lambda_2\Gamma_1^2 - 2\lambda_3\sum_{j=1}^{N+M-1}\Theta_{1,j}^2 & \ldots & 2\gamma_{1,L}\lambda_1 - \alpha\lambda_2\Gamma_1\Gamma_L - 2\lambda_3\sum_{j=1}^{N+M-1}\Theta_{1,j}\Theta_{L,j} & 0 \\ 2\gamma_{2,1}\lambda_1 - \alpha\lambda_2\Gamma_2\Gamma_1 - 2\lambda_3\sum_{j=1}^{N+M-1}\Theta_{2,j}\Theta_{1,j} & \ldots & 2\gamma_{2,L}\lambda_1 - \alpha\lambda_2\Gamma_2\Gamma_L - 2\lambda_3\sum_{j=1}^{N+M-1}\Theta_{2,j}\Theta_{L,j} & 0 \\ \vdots & & & \vdots \\ 2\gamma_{L,1}\lambda_1 - \alpha\lambda_2\Gamma_L\Gamma_1 - 2\lambda_3\sum_{j=1}^{N+M-1}\Theta_{L,j}\Theta_{1,j} & \ldots & -2\gamma_{L,L}\lambda_1 - \alpha\lambda_2\Gamma_L^2 - 2\lambda_3\sum_{j=1}^{N+M-1}\Theta_{L,j}^2 & 0 \\ 0 & \ldots & 0 & 0 \end{bmatrix} \tag{31}$$

$$\mathbf{B}_k = \begin{bmatrix} \lambda_1\left(\gamma_{0,1} + \frac{\eta_s}{\eta_d}\Gamma_1\right) + \lambda_2\left(\omega\sum_{j=1}^{L}\gamma_{1,j} - \alpha\Gamma_0\Gamma_1\right) - 2\lambda_3\sum_{j=1}^{N+M-1}\Theta_{0,j}\Theta_{1,j} \\ \vdots \\ \lambda_1(\gamma_{0,L} + \frac{\eta_s}{\eta_d}\Gamma_L) + \lambda_2\left(\omega\sum_{j=1}^{L}\gamma_{L,j} - \alpha\Gamma_0\Gamma_L\right) - 2\lambda_3\sum_{j=1}^{N+M-1}\Theta_{0,j}\Theta_{L,j} \\ -(c_k + \eta_s\eta_c)\lambda_1 \end{bmatrix} \tag{32}$$

$$\begin{aligned} r_k = {}& \lambda_1\eta_s(\Gamma_0/\eta_d - I_k - \eta_c u_k) + \lambda_2\left(\omega\Gamma_0 - \frac{\alpha}{2}\left(\Gamma_0^2 + \sum_{j=1}^{L}\sigma_{k,j}^2\right)\right) \\ & - \lambda_3\left(\sum_{j=1}^{N+M-1}\Theta_{0,j}^2 + \lambda_3\sum_{j=1}^{N+M-1}\sum_{i=1}^{L} b_{j,a_i}^2\sigma_{k,j}^2\right) + \mathbb{E}_{u_{k+1}}\{J_{k+1}(I_{k+1}, u_{k+1})\} \end{aligned} \tag{33}$$

TABLE I
SIMULATION PARAMETERS

Coefficient	Description	Unit	Value
N	Number of horizons	-	24
E	Energy storage capacity	MWh	200
λ_1	Weight for profit	-	0 to 1
λ_2	Weight for customer satisfaction	-	0 to 1
λ_3	Weight for impact	-	0 to 1
ζ	Revenue safeguard probability	-	0.2
α	Shape parameter	-	5e-5
ω	Shape parameter	-	0.01
η_s	Unit storage cost	$/MWh	0 to 4
η_c	Energy storage charging efficiency	-	0.9
η_d	Energy storage discharging efficiency	-	0.9
ρ_0	Knee point threshold	-	1

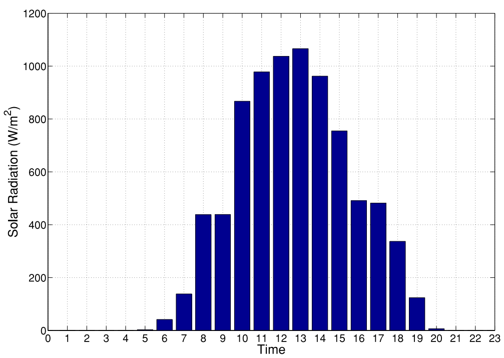

Fig. 4. Typical Daily Solar Radiation.

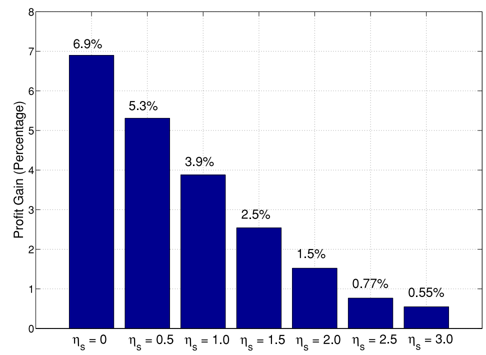

Fig. 5. SDP Profit Increase Percentage.

data from PJM [62] to represent the real time wholesale price forecasting in the simulations, but other forecasting approaches can be used. In addition, we assume that the charging service provider procures electricity at a single locational marginal price (LMP). We use solar power to represent the renewable energy source. The solar radiation data is from National Renewable Energy Laboratory (NREL) [63], and the typical daily solar radiation is depicted in Fig. 4. Note that solar radiation begins at 6:00 am and ends at 8:00 pm. Additionally, we assume that solar cell efficiency is 20%. We use IEEE 57 Bus Test case for the power network in our simulations [64].

A. SDP Algorithm Versus Greedy Algorithm

The greedy algorithm aims to optimize the current planning horizon without considering the future. We use the greedy algorithm as a benchmark, to which we compare the SDP algorithm in terms of profitability. The profit percentage gain of SDP algorithm compared to greedy algorithm is shown in Fig. 5. The simulation reveals that the SDP algorithm can achieve up to 7% profit gain compared to the greedy algorithm. The reason why SDP is able to obtain a higher profit is that it fully exploits the information of day-ahead wholesale electricity prices and renewable energy prediction, and makes decisions to optimize the aggregated utility over multiple horizons. However, the greedy algorithm lacks a forward-looking vision, which solely maximizes the utility of the current horizon. As far as the computational complexity is concerned, greedy algorithm has a linear time complexity with $O(K)$, and SDP has a quadratic time complexity with $O(K^2)$, where K is the number of planning horizons. This is because the greedy algorithm only involves one loop from horizon 0 to horizon 23. However, the SDP algorithm has two loops with the outer loop starting from horizon 0 to horizon 23 and the inner loop for backward recursive SDP calculation. In essence, the SDP algorithm trades complexity for a higher profit.

B. Aggressive or Conservative Electricity Procurement Strategy

An electricity storage enables the charging service provider to store the intermittent renewable energy or excessive electricity when the wholesale price is low, and sell it to EVs when the wholesale price is high. In this subsection, we analyse how this "buy low and sell high" strategy will change when the unit storage cost ($\eta_s = 0$ to 4) changes. In Fig. 6, electricity procurement strategies with different unit storage costs are depicted in the first four subplots, and the last subplot shows the real time wholesale electricity prices. We can make three observations: (1) From 8:00 to 16:00, the service provider tends to procure less electricity from the wholesale market because of renewable energy generation at this period of time, and (2) The service provider tends to procure more

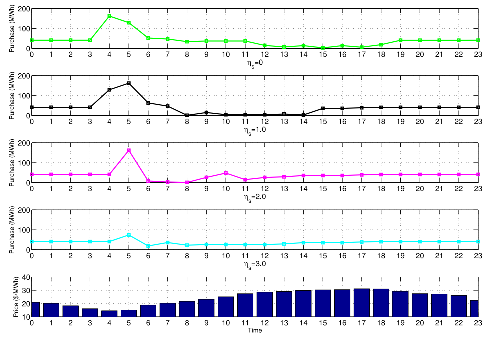

Fig. 6. Electricity Procurement with Different Storage Cost.

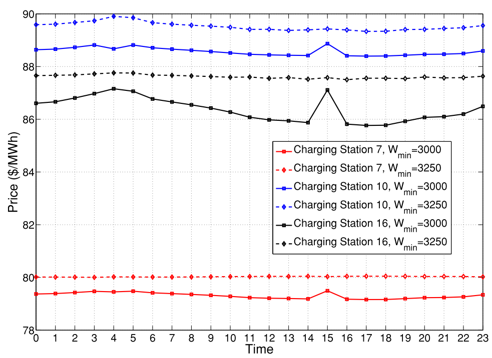

Fig. 7. Charging Prices with Different $W_{\min}$.

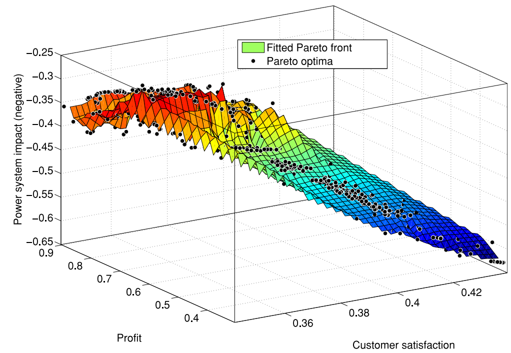

Fig. 8. Pareto Front.

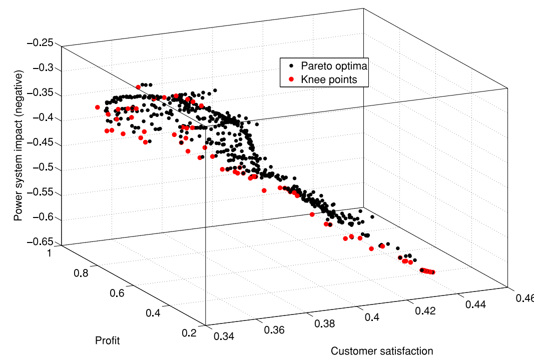

Fig. 9. Pareto Front with Knee Points.

electricity during the low wholesale price period (from 3:00 to 6:00) and procure less electricity during the high wholesale price period (from 11:00 to 17:00), and (3) When η_s is small, the service provider becomes aggressive in electricity procurement during low price period, and when η_s is large, it becomes more conservative.

C. Charging Price With Safeguard of Profit

In the simulation, we investigate the interplay between charging prices and the safeguard of profit. From Fig. 7, we note that the charging prices increase as the profit threshold $W_{\min}$ increases. According to Eq. (24), we must ensure the probability ζ does not change even if $W_{\min}$ increases. In other words, $(W_{\min} - \mathbf{X}_k^{\mathrm{T}}\mathbf{A}\mathbf{X}_k - \mathbf{B}^{\mathrm{T}}\mathbf{X}_k - t_k)/(\sqrt{\sum_{j=1}^{L}(p_{kj} + \eta_s/\eta_d)^2\sigma_{kj}^2 + \eta_s^2\sigma_w^2})$ should not change as $W_{\min}$ increases. The simulation results show that the charging service provider ends up raising charging prices to ensure the probability ζ.

D. Pareto Optima and Knee Points

We need to simultaneously maximize multiple objectives — profit, customer satisfaction, and the negative of impact on power grid. Each point in Fig. 8 is a Pareto optimum in which it is impossible to increase any one individual objective without decreasing at least one of the other objectives [41]. The Pareto front is obtained by using the linear interpolation fitting method [65].

Knee points in the Pareto front provide the best trade-off among multiple objectives, which yield largest improvement per unit degradation. Following the metric discussed in [66] and [67], we define $\rho(Y_i, S)$ to represent the least improvement per unit degradation by replacing any other Pareto optima in S with Y_i. The entries in $Y_i = [y_{1i}, y_{2i}, y_{3i}]^{\mathrm{T}}$ represent the profit, the customer satisfaction, and the impact on power grid, respectively.

$$\rho(Y_i, S) = \min_{Y_j \in S, j \neq i} \frac{\sum_{k=1}^{3} \max\left(0, y_{ki} - y_{kj}\right)}{\sum_{k=1}^{3} \max\left(0, y_{kj} - y_{ki}\right)}. \quad (36)$$

Then we set a threshold ρ_0 to select the knee points as follows,

$$S_{\text{knee}}^{\rho_0} = \{Y_i | \rho(Y_i, S) > \rho_0;\ Y_i \in S\}. \quad (37)$$

We use $\rho = 1$ in the simulations. The knee points are marked in red in Fig. 9. We notice that there are several knee regions among the Pareto optima, which reflect different preference over the three objectives — profit, customer satisfaction, and the impact on power grid.

E. Interplays Between Profit, Customer Satisfaction, and Impact on Power Grid

The projection of Pareto optima on the Profit-Customer plane is plotted in Fig. 10. We observe that customer satisfaction decreases when profit increases. This is because the charging service provider raises charging prices to decrease the total charging demand. The decreased total charging demand leads to a decreased customer satisfaction. However, the net effect of raising charging prices is that the service provider achieves a higher profit. Therefore, the service provider should strike a balance between the two competing objectives of profit and customer satisfaction.

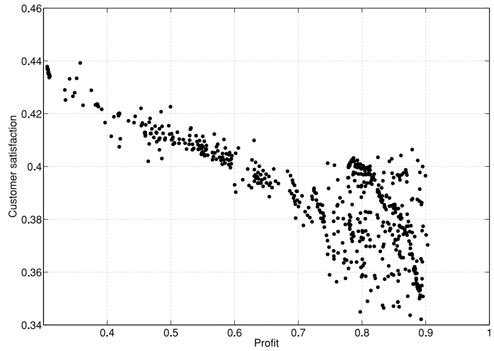

Fig. 10. Profit vs Customer Satisfaction.

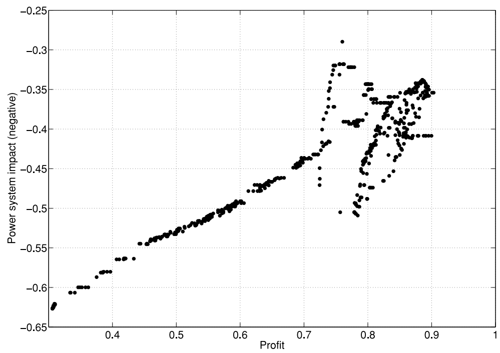

Fig. 11. Profit vs Impact on Power Grid.

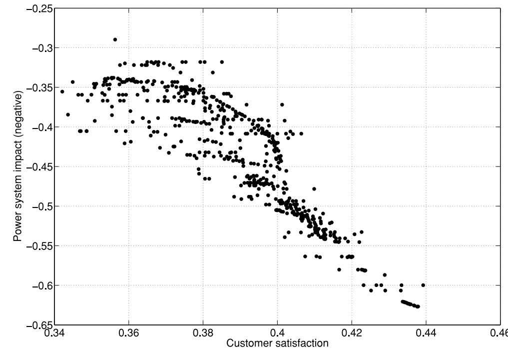

Fig. 12. Customer Satisfaction vs Impact on Power Grid.

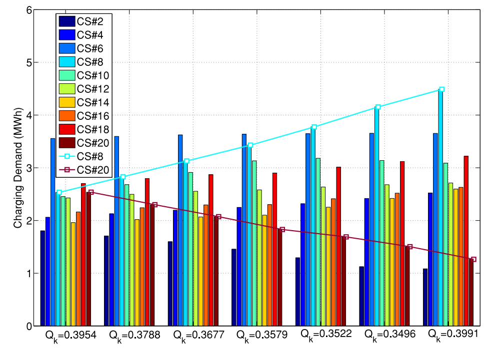

Fig. 13. Charging Demand Redistribution with Different Impacts.

The projection of Pareto optima on the Profit-Impact plane is plotted in Fig. 11. It turns out that the impact and the profit are not competing objectives since the impact on power grid decreases when profit increases. The increased charging prices cause a decrease in total charging demand, relieving the stress on power grid. However, the profit is improved even though the total charging demand decreases.

Fig. 12 shows the projection of Pareto optima on the Customer-Impact plane. Note that customer satisfaction and the impact are competing objectives since the impact on power grid increases as customer satisfaction increases. It is obvious that customer satisfaction and impact on power grid are both related to the total charging demand. According to Eq. (2), customer satisfaction increases when the total charging demand increases. However, the increased charging demand will inevitably pose a heavier stress on the power grid.

F. Spatial Charging Demand Versus Impact on Power Grid

The relationship between spatial charging demand and impact on power grid is shown in Fig. 13. Due to limited space, we only plotted the charging stations with even indices. We observe that as the impact on power grid (Q_k) decreases, the charging demands of Charging Station #2 (CS#2) and Charging Station #20 (CS#20) decrease while the charging demands of other charging stations increase. This is because the PQ buses feeding CS#2 and CS#20 have larger active power sensitivity metric S_i^{Ac} than the others. The active power sensitivity for charging stations with even indices are $[0.80, 0.61, 0.33, 0.17, 0.31, 0.29, 0.22, 0.60, 0.29, 1.33]$. Note that CS#8 has the smallest active power sensitivity 0.17, its charging demand increases very fast as the impact decreases. While CS#20 has the largest active power sensitivity 1.33, its charging demand decreases fast. Thus, the service provider has to shift the charging demands from the PQ buses with large S_i^{Ac} to those with small S_i^{Ac} to reduce the impact on power grid.

VII. CONCLUSION

This paper proposes a multi-objective optimization framework for EV charging service provider to determine retail charging prices and appropriate amount of electricity to purchase from the real time wholesale market. A linear regression model is employed to estimate EV charging demands. To cope with multiple uncertainties, SDP algorithm is applied to simplify the optimization problem. Compared to greedy algorithm (benchmark), SDP algorithm can make a higher profit at the cost of increased algorithm complexity. A lost-cost electricity storage is beneficial for the service provider to harvest the intermittent renewable energy and exert the "buy low and sell high" strategy to improve profits. In addition, the service provider can shift charging demands from high-sensitive buses to low-sensitive buses to alleviate the impact on power grid by changing charging prices.

REFERENCES

[1] A. Simpson, "Cost-benefit analysis of plug-in hybrid electric vehicle technology," in *Proc. 22nd Int. Battery Hybrid Fuel Cell Elect. Veh. Symp. Exhibit. (EVS)*, Yokohama, Japan, 2006, pp. 1–15.

[2] M. Hajian, H. Zareipour, and W. D. Rosehart, "Environmental benefits of plug-in hybrid electric vehicles: The case of Alberta," in *Proc. IEEE Power Energy Soc. Gener. Meeting (PES)*, Calgary, AB, Canada, 2009, pp. 1–6.

[3] R. Sioshansi and P. Denholm, "Emissions impacts and benefits of plug-in hybrid electric vehicles and vehicle-to-grid services," *Environ. Sci. Technol.*, vol. 43, no. 4, pp. 1199–1204, 2009.

[4] C. Luo, Y.-F. Huang, and V. Gupta, "A consumer behavior based approach to multi-stage EV charging station placement," in *Proc. IEEE 81st Veh. Technol. Conf. (VTC Spring)*, Glasgow, U.K., 2015, pp. 1–6.

[5] C. Luo, Y.-F. Huang, and V. Gupta, "Placement of EV charging stations—Balancing benefits among multiple entities," *IEEE Trans. Smart Grid*, vol. 8, no. 2, pp. 759–768, Mar. 2017.

[6] Z. Yi and P. H. Bauer, "Optimization models for placement of an energy-aware electric vehicle charging infrastructure," *Transp. Res. E Logistics Transp. Rev.*, vol. 91, no. 1, pp. 227–244, Jul. 2016.

[7] A. Y. S. Lam, Y.-W. Leung, and X. Chu, "Electric vehicle charging station placement: Formulation, complexity, and solutions," *IEEE Trans. Smart Grid*, vol. 5, no. 6, pp. 2846–2856, Nov. 2014.

[8] Z. Yi and P. H. Bauer, "Spatiotemporal energy demand models for electric vehicles," *IEEE Trans. Veh. Technol.*, vol. 65, no. 3, pp. 1030–1042, Mar. 2016.

[9] Y. Guo, X. Liu, Y. Yan, N. Zhang, and W. Su, "Economic analysis of plug-in electric vehicle parking deck with dynamic pricing," in *Proc. IEEE Power Energy Soc. Gener. Meeting*, National Harbor, MD, USA, 2014, pp. 1–5.

[10] Y. Guo, J. Xiong, S. Xu, and W. Su, "Two-stage economic operation of microgrid-like electric vehicle parking deck," *IEEE Trans. Smart Grid*, vol. 7, no. 3, pp. 1703–1712, May 2016.

[11] J. M. Foster and M. C. Caramanis, "Optimal power market participation of plug-in electric vehicles pooled by distribution feeder," *IEEE Trans. Power Syst.*, vol. 28, no. 3, pp. 2065–2076, Aug. 2013.

[12] S. Han, S. Han, and K. Sezaki, "Development of an optimal vehicle-to-grid aggregator for frequency regulation," *IEEE Trans. Smart Grid*, vol. 1, no. 1, pp. 65–72, Jun. 2010.

[13] E. Sortomme and M. A. El-Sharkawi, "Optimal charging strategies for unidirectional vehicle-to-grid," *IEEE Trans. Smart Grid*, vol. 2, no. 1, pp. 131–138, Mar. 2011.

[14] S. Beer *et al.*, "An economic analysis of used electric vehicle batteries integrated into commercial building microgrids," *IEEE Trans. Smart Grid*, vol. 3, no. 1, pp. 517–525, Mar. 2012.

[15] Y. Han, Y. Chen, F. Han, and K. J. R. Liu, "An optimal dynamic pricing and schedule approach in V2G," in *Proc. Asia–Pac. Signal Inf. Process. Assoc. Annu. Summit Conf. (APSIPA ASC)*, Hollywood, CA, USA, 2012, pp. 1–8.

[16] A. Ovalle, A. Hably, and S. Bacha, "Optimal management and integration of electric vehicles to the grid: Dynamic programming and game theory approach," in *Proc. IEEE Int. Conf. Ind. Technol. (ICIT)*, Seville, Spain, 2015, pp. 2673–2679.

[17] H. K. Nguyen and J. B. Song, "Optimal charging and discharging for multiple PHEVs with demand side management in vehicle-to-building," *J. Commun. Netw.*, vol. 14, no. 6, pp. 662–671, Dec. 2012.

[18] R. Couillet, S. M. Perlaza, H. Tembine, and M. Debbah, "Electrical vehicles in the smart grid: A mean field game analysis," *IEEE J. Sel. Areas Commun.*, vol. 30, no. 6, pp. 1086–1096, Jul. 2012.

[19] Q. Yan, I. Manickam, M. Kezunovic, and L. Xie, "A multi-tiered real-time pricing algorithm for electric vehicle charging stations," in *Proc. IEEE Transp. Electrification Conf. Expo (ITEC)*, Dearborn, MI, USA, 2014, pp. 1–6.

[20] D. Ban, G. Michailidis, and M. Devetsikiotis, "Demand response control for PHEV charging stations by dynamic price adjustments," in *Proc. IEEE PES Innov. Smart Grid Technol. (ISGT)*, Washington, DC, USA, 2012, pp. 1–8.

[21] N. Rahbari-Asr, M.-Y. Chow, Z. Yang, and J. Chen, "Network cooperative distributed pricing control system for large-scale optimal charging of PHEVs/PEVs," in *Proc. 39th Annu. Conf. IEEE Ind. Electron. Soc. (IECON)*, Vienna, Austria, 2013, pp. 6148–6153.

[22] E. C. Özelkan, Á. Galambosi, E. Fernández-Gaucherand, and L. Duckstein, "Linear quadratic dynamic programming for water reservoir management," *Appl. Math. Model.*, vol. 21, no. 9, pp. 591–598, 1997.

[23] A. L. Kerr, "Stochastic utility maximising dynamic programming applied to medium-term reservoir management," Ph.D. dissertation, Manag. Netw. Digit. Library, Univ. Canterbury, Christchurch, New Zealand, 2003.

[24] L. Jia and L. Tong, "Dynamic pricing and distributed energy management for demand response," *IEEE Trans. Smart Grid*, vol. 7, no. 2, pp. 1128–1136, Mar. 2016.

[25] R. Huisman, C. Huurman, and R. Mahieu, "Hourly electricity prices in day-ahead markets," *Energy Econ.*, vol. 29, no. 2, pp. 240–248, 2007.

[26] G. Hamoud and I. Bradley, "Assessment of transmission congestion cost and locational marginal pricing in a competitive electricity market," *IEEE Trans. Power Syst.*, vol. 19, no. 2, pp. 769–775, May 2004.

[27] M. Ventosa, Á. Baíllo, A. Ramos, and M. Rivier, "Electricity market modeling trends," *Energy Policy*, vol. 33, no. 7, pp. 897–913, 2005.

[28] P. Yang, G. Tang, and A. Nehorai, "A game-theoretic approach for optimal time-of-use electricity pricing," *IEEE Trans. Power Syst.*, vol. 28, no. 2, pp. 884–892, May 2013.

[29] M. Fahrioglu and F. L. Alvarado, "Designing cost effective demand management contracts using game theory," in *Proc. IEEE Power Eng. Soc. Winter Meeting*, vol. 1. New York, NY, USA, 1999, pp. 427–432.

[30] R. Faranda, A. Pievatolo, and E. Tironi, "Load shedding: A new proposal," *IEEE Trans. Power Syst.*, vol. 22, no. 4, pp. 2086–2093, Nov. 2007.

[31] H. H. Gossen, *The Laws of Human Relations and the Rules of Human Action Derived Therefrom*. Cambridge, MA, USA: MIT Press, 1983.

[32] H. Turker, S. Bacha, D. Chatroux, and A. Hably, "Low-voltage transformer loss-of-life assessments for a high penetration of plug-in hybrid electric vehicles (PHEVs)," *IEEE Trans. Power Del.*, vol. 27, no. 3, pp. 1323–1331, Jul. 2012.

[33] K. N. Kumar, B. Sivaneasan, P. L. So, and D. Z. W. Wang, "Methodology for optimizing the number of electric vehicles deployed under a smart grid," in *Proc. 39th Annu. Conf. IEEE Ind. Electron. Soc. (IECON)*, Vienna, Austria, 2013, pp. 4647–4652.

[34] J. A. P. Lopes, F. J. Soares, and P. M. R. Almeida, "Integration of electric vehicles in the electric power system," *Proc. IEEE*, vol. 99, no. 1, pp. 168–183, Jan. 2011.

[35] K. Schneider, C. Gerkensmeyer, M. Kintner-Meyer, and R. Fletcher, "Impact assessment of plug-in hybrid vehicles on Pacific Northwest distribution systems," in *Proc. IEEE Power Energy Soc. Gener. Meeting Convers. Del. Elect. Energy 21st Century*, Pittsburgh, PA, USA, 2008, pp. 1–6.

[36] W. Su, J. Wang, K. Zhang, and M.-Y. Chow, "Framework for investigating the impact of PHEV charging on power distribution system and transportation network," in *Proc. 38th Annu. Conf. IEEE Ind. Electron. Soc. (IECON)*, Montreal, QC, Canada, 2012, pp. 4735–4740.

[37] P. Kundur, *Power System Stability and Control*, 1st ed. New York, NY, USA: McGraw-Hill, 1994.

[38] RENAC Online Academy. *ReGrid: Frequency and Voltage Regulation in Electrical Grids*. Accessed on Oct. 2015. [Online]. Available: http://docplayer.net/6038884-Regrid-frequency-and-voltage-regulation-in-electrical-grids.html

[39] C. Zhao, U. Topcu, and S. H. Low, "Optimal load control via frequency measurement and neighborhood area communication," *IEEE Trans. Power Syst.*, vol. 28, no. 4, pp. 3576–3587, Nov. 2013.

[40] M. R. V. Moghadam, R. Zhang, and R. T. B. Ma, "Distributed frequency control via randomized response of electric vehicles in power grid," *IEEE Trans. Sustain. Energy*, vol. 7, no. 1, pp. 312–324, Jan. 2016.

[41] C.-L. Hwang and A. S. M. Masud, *Multiple Objective Decision Making—Methods and Applications*. Heidelberg, Germany: Springer, 1979.

[42] K. Miettinen, *Nonlinear Multiobjective Optimization*. New York, NY, USA: Springer, 1999.

[43] I. Y. Kim and O. L. de Weck, "Adaptive weighted sum method for multiobjective optimization: A new method for Pareto front generation," *Struct. Multidiscipl. Optim.*, vol. 31, no. 2, pp. 105–116, 2006.

[44] R. Christensen, *Plane Answers to Complex Questions: The Theory of Linear Models*, 3rd ed. New York, NY, USA: Springer, 2002.

[45] A. Dobson and A. Barnett, *An Introduction to Generalized Linear Models*, 3rd ed. Hoboken, NJ, USA: CRC Press, 2008.

[46] J. Proakis, *Digital Signal Processing*, 4th ed. Upper Saddle River, NJ, USA: Prentice-Hall, 2007.

[47] J. Lu and R. Niu, "False information injection attack on dynamic state estimation in multi-sensor systems," in *Proc. 17th Int. Conf. Inf. Fusion (FUSION)*, Salamanca, Spain, 2014, pp. 1–8.

[48] S. Frank and S. Rebennack, "A primer on optimal power flow: Theory, formulation, and practical examples," *IDEAS Working Paper Series From RePEc*, 2012.

[49] L. Landberg, "Short-term prediction of the power production from wind farms," *J. Wind Eng. Ind. Aerodyn.*, vol. 80, no. 1, pp. 207–220, 1999.

[50] M. Lange and U. Focken, *Physical Approach to Short-Term Wind Power Prediction*. Berlin, Germany: Springer, 2006.

[51] Y.-Z. Li, R. Luan, and J.-C. Niu, "Forecast of power generation for grid-connected photovoltaic system based on grey model and Markov chain," in *Proc. 3rd IEEE Conf. Ind. Electron. Appl.*, Singapore, 2008, pp. 1729–1733.

[52] E. Izgia, A. Öztopalb, B. Yerlib, M. K. Kaymakb, and A. D. Şahin, "Short–mid-term solar power prediction by using artificial neural networks," *Solar Energy*, vol. 86, no. 2, pp. 725–733, 2012.

[53] G. Giebel, L. Landberg, A. Joensen, and H. Madsen, "The Zephyr project: The next generation prediction system," in *Proc. Eur. Wind Energy Assoc. Conf.*, 2001, pp. 777–780.

[54] J. R. Norris, *Markov Chain*. Cambridge, U.K.: Cambridge Univ. Press, 1997.

[55] P. Bremaud, *Markov Chains: Gibbs Fields, Monte Carlo Simulation, and Queues*. New York, NY, USA: Springer, 1999.

[56] Y. Ji, J. Kim, R. J. Thomas, and L. Tong, "Forecasting real-time locational marginal price: A state space approach," in *Proc. Asilomar Conf. Signals Syst. Comput.*, Pacific Grove, CA, USA, 2013, pp. 379–383.

[57] R. Weron, "Electricity price forecasting: A review of the state-of-the-art with a look into the future," *Int. J. Forecasting*, vol. 30, no. 4, pp. 1030–1081, 2014.

[58] J. Lu, R. Niu, and P. Han, "Optimal space-time attacks on system state estimation under a sparsity constraint," in *Proc. SPIE Sensors Syst. Space Appl. IX*, Baltimore, MD, USA, 2016, Art. no. 98380H.

[59] D. Bertsekas, *Dynamic Programming and Optimal Control*, 2nd ed. Belmont, MA, USA: Athena Sci., 2000.

[60] Tesla.com. *Powerwall—Energy Storage for a Sustainable Home*. Accessed on Oct. 6, 2016. [Online]. Available: https://www.tesla.com/powerwall

[61] EosEnergy.com. *Products: Eos Aurora*. Accessed on Oct. 6, 2016. [Online]. Available: http://www.eosenergystorage.com/products/

[62] PJM.com. *Daily Day-Ahead LMP*. Accessed on Oct. 17, 2016. [Online]. Available: http://www.pjm.com/markets-and-operations/energy/day-ahead/lmpda.aspx

[63] E. McKenna and A. Andreas, "South Park mountain data: South Park, Colorado (data)," NREL, Golden, CO, USA, Tech. Rep. DA-5500-56521, 1997. [Online]. Available: http://dx.doi.org/10.5439/1052562

[64] I. Dabbagchi and R. Christie. *Power Systems Test Case Archive: 57 Bus Power Flow Test Case*. Accessed on Oct. 5, 2016. [Online]. Available: http://www2.ee.washington.edu/research/pstca/pf57/pg_tca57bus.htm

[65] P. J. Davis, *Interpolation and Approximation*. New York, NY, USA: Blaisdell, 1963.

[66] L. Rachmawati and D. Srinivasan, "Multiobjective evolutionary algorithm with controllable focus on the knees of the Pareto front," *IEEE Trans. Evol. Comput.*, vol. 13, no. 4, pp. 810–824, Aug. 2009.

[67] X. Zhang, Y. Zhou, Q. Zhang, V. C. S. Lee, and M. Li, "Multi-objective optimization of barrier coverage with wireless sensors," in *Evolutionary Multi-Criterion Optimization*. Cham, Switzerland: Springer, 2015, pp. 557–572.

Chao Luo received the B.Eng. (with Distinction) degree in communication engineering from the Harbin Institute of Technology, China, in 2012. He is currently pursuing the Ph.D. degree in electrical engineering with the University of Notre Dame, USA. His research interests include electric vehicle integration into power system, machine learning in smart grid, power system architecture, and electricity market.

Yih-Fang Huang (S'80–M'82–SM'94–F'95) received the B.S.E.E. degree from National Taiwan University, the M.S.E.E. degree from the University of Notre Dame, and the Ph.D. from Princeton University. He is a Professor of the Department of Electrical Engineering and the Senior Associate Dean of College of Engineering, University of Notre Dame. He served as the Chair of the Electrical Engineering Department, University of Notre Dame from 1998 to 2006. His research interests focus on theory and applications of statistical signal detection and estimation and adaptive signal processing.

He was a recipient of the Toshiba Fellowship in 1993 and the Fulbright-Nokia Scholarship for Lectures/Research at Helsinki University of Technology in Finland (which is currently Aalto University) in 2007. He was a Toshiba Visiting Professor with Waseda University, Tokyo, Japan. He was a Visiting Professor with the Munich University of Technology, Germany, for three months, in 2007.

Dr. Huang was a recipient of the Golden Jubilee Medal of the IEEE Circuits and Systems Society in 1999, the Presidential Award at the University of Notre Dame, in 2003, the Electrical Engineering Department's Outstanding Teacher Award in 1994 and 2011, the Rev. Edmund P. Joyce, CSC Award for Excellence in Undergraduate Teaching in 2011, and the College of Engineering's Teacher of the Year Award in 2013. He served as the Vice President from 1997 to 1998 and was a Distinguished Lecturer for the same society from 2000 to 2001.

Vijay Gupta received the B.Tech. degree from the Indian Institute of Technology, Delhi, and the M.S. and Ph.D. degrees from the California Institute of Technology, all in Electrical Engineering. He is a Professor with the Department of Electrical Engineering, University of Notre Dame. Prior to joining Notre Dame, he also served as a Research Associate with the Institute for Systems Research, University of Maryland, College Park. His research interests include cyber-physical systems, distributed estimation, detection and control, and, in general, the interaction of communication, computation, and control. He was a recipient of the NSF CAREER Award in 2009 and the Donald P. Eckman Award from the American Automatic Control Council in 2013.